Modeling the Oxygen Activation Chemistry of Methane Monooxygenase and Ribonucleotide Reductase

LAWRENCE QUE, JR.,* AND YANHONG DONG

Department of Chemistry, University of Minnesota, Minneapolis, Minnesota 55455

Received June 1, 1995

Introduction

The activation of dioxygen has long fascinated researchers in many fields because of its fundamental and technological significance.[1] In bioinorganic chemistry, much effort has focused on the mechanisms of heme enzymes, particularly cytochrome P450; an oxoiron(IV) porphyrin radical (formally Fe^{V}) species has emerged as the likely oxidant in many reactions.[2] More recently oxygen-activating enzymes with carboxylate-bridged non-heme diiron sites have also attracted intense interest.[3] Prominent among these are methane monooxygenase (MMO[4]), which converts methane to methanol,[5] and ribonucleotide reductase (RNR), which is a key enzyme in the biosynthesis of DNA.[6] MMO consists of three components, a hydroxylase, a reductase, and a coupling protein, and the diiron site responsible for dioxygen activation and alkane hydroxylation resides in the hydroxylase component (MMOH). RNR, on the other hand, consists of R1 and R2 components. Ribonucleotide reduction on R1 is initiated by a stable Tyr radical found in R2; the tyrosyl radical is formed by dioxygen activation on the diiron site in R2.

Crystal structures of MMOH[7,8] and RNR R2,[9,10] as well as the invertebrate dioxygen carrier hemerythrin (Hr),[11] which also has a carboxylate-bridged non-heme diiron site,[12] are now available in both the diiron(II) and diiron(III) oxidation states (Figure 1). These structures together with a variety of spectroscopic and biomimetic studies[3a,11c,13] have contributed greatly to our knowledge of these diiron active sites. It is clear from a comparison of these structures that the active site of Hr differs significantly from those of the other two, possibly reflecting its different function. The active site of Hr consists of a triply bridged diiron core that is coordinated by five terminal His ligands. Dioxygen binds at the vacant site in the deoxy form, and the proton from the hydroxo bridge shifts to the bound O_2 as two electrons from the diiron(II) core are transferred to O_2, reducing it to the peroxide oxidation state (Figure 1). The minimal structural changes associated with the diiron core upon oxygenation and deoxygenation are consistent with its reversible dioxygen binding function, which requires that the deoxy and oxy forms be in thermodynamic equilibrium.

MMOH and RNR R2, on the other hand, have very similar active sites, which are carboxylate-rich relative to that of Hr. In the reduced enzymes, each iron(II) ion is terminally coordinated by one histidine and one carboxylate and bridged to the other iron(II) ion by two carboxylates. Thus both iron(II) ions have available sites for O_2 to bind. Upon oxidation, one of the bridging carboxylates shifts to a terminal position; such carboxylate shifts[14] may play an important but as yet undefined role in oxygen activation.

There has been recent significant progress in understanding the dioxygen activation mechanisms of these non-heme diiron enzymes. Transient intermediates have been observed in rapid kinetic studies of the reactions of the diiron(II) forms of MMOH[15,16] and RNR R2[17] with O_2 (Figure 2). For MMOH, the

Lawrence Que, Jr., did his undergraduate work at Ateneo de Manila University (B.S. 1969) and pursued graduate studies at the University of Minnesota under Professor Louis H. Pignolet (Ph.D. 1973). After postdoctoral stints with Professors Richard H. Holm at MIT and Eckard Münck at the University of Minnesota, he joined the Cornell University faculty as an assistant professor of chemistry. In 1983 he returned to the University of Minnesota, where he is now professor of chemistry and co-director of the Center for Metals in Biocatalysis. His research has focused on the interface between inorganic chemistry and biology with particular emphasis on understanding the mechanisms of dioxygen activation by non-heme iron enzymes and synthesizing structural, spectroscopic, and functional models of these enzymes.

Yanhong Dong received her B.S. (1982) and Ph.D. (1989) in chemistry from Nanjing University. For her Ph.D., she worked on platinum–DNA interactions under the direction of Professors Anbang Dai and Wenxia Tang. She is presently a postdoctoral associate at the University of Minnesota in the laboratory of Professor Lawrence Que, Jr. She has synthesized and characterized a number of novel intermediates that are relevant to the dioxygen activation mechanisms of non-heme iron enzymes.

(1) Valentine, J. S., Foote, C. S., Greenberg, A., Liebman, J. F., Eds. *Active Oxygen in Biochemistry*; Chapman and Hall: London, 1995.
(2) Ortiz de Montellano, P. R., Ed. *Cytochrome P-450. Structure, Mechanism and Biochemistry*; Plenum Press: New York, 1986.
(3) (a) Feig, A. L.; Lippard, S. J. *Chem. Rev.* **1994**, *94*, 759−805. (b) Que, L., Jr. In *Bioinorganic Catalysis*; Reedijk, J., Ed.; Marcel Dekker, Inc.: New York, 1993; pp 347−393.
(4) Abbreviations used: acac = 2,4-pentanedione (acetylacetone); BIPhMe = bis(1-methylimidazol-2-yl)phenylmethoxymethane; Bzim = benzimidazole; Cl_4Cat = tetrachlorocatecholate; EDTA = ethylenediaminetetraacetate; Hr = hemerythrin; MMO = methane monooxygenase; MMOH = the hydroxylase component of methane monooxygenase; N-Et-HPTB = 1,3-bis(*N*,*N*-bis(1-ethylbenzimidazol-2-yl)amino)-2-hydroxypropane; OAc = acetate; OBz = benzoate; OEP = octaethylporphinate dianion; RNR R2 = the R2 protein of ribonucleotide reductase; Me_3TACN = 1,4,7-trimethyl-1,4,7-triazacyclononane; TPA = tris(2-pyridylmethyl)-amine; 5-Et_3-TPA = tris((5-ethyl-2-pyridyl)methyl)amine; 5-Me_3-TPA = tris(5-methyl-2-pyridylmethyl)amine; 6-Me-TPA = *N*-((6-methyl-2-pyridyl)methyl)-*N*,*N*-bis(2-pyridylmethyl)amine; 6-Me_3-TPA = tris((6-methyl-2-pyridyl)methyl)amine; tpdb = 1,4-bis(*N*,*N*-bis(2-pyridylmethyl)-amino)-2-hydroxybutane; Tp^{iPr2} = hydrotris(3,5-diisopropyl-1-pyrazolyl)borate; TPP = tetraphenylporphinate dianion.
(5) Lipscomb, J. D. *Annu. Rev. Microbiol.* **1994**, *48*, 371−399.
(6) (a) Stubbe, J. *Adv. Enzymol.* **1989**, *63*, 349−419. (b) Fontecave, M.; Nordlund, P.; Eklund, H.; Reichard, P. *Adv. Enzymol.* **1992**, *65*, 147−183.
(7) Rosenzweig, A. C.; Frederick, C. A.; Lippard, S. J.; Nordlund, P. *Nature* **1993**, *366*, 537−543.
(8) Rosenzweig, A. C.; Nordlund, P.; Takahara, P. M.; Frederick, C. A.; Lippard, S. J. *Chem. Biol.* **1995**, *2*, 409−418.
(9) (a) Nordlund, P.; Sjöberg, B.-M.; Eklund, H. *Nature* **1990**, *345*, 593−598. (b) Nordlund, P.; Eklund, H. *J. Mol. Biol.* **1993**, *232*, 123−164.
(10) (a) Atta, M.; Nordlund, P.; Åberg, A.; Eklund, H.; Fontecave, M. *J. Biol. Chem.* **1992**, *267*, 20682−20688. (b) Åberg, A. Ph.D. Thesis, Stockholm University, 1993.
(11) (a) Wilkins, P. C.; Wilkins, R. G. *Coord. Chem. Rev.* **1987**, *79*, 195−214. (b) Wilkins, R. G. *Chem. Soc. Rev.* **1992**, 171−178. (c) Sanders-Loehr, J. In *Iron Carriers and Iron Proteins*; Loehr, T. M., Ed.; VCH: Weinheim, 1989; pp 373−467.
(12) Stenkamp, R. E. *Chem. Rev.* **1994**, *94*, 715−726.
(13) (a) Que, L., Jr.; True, A. E. *Prog. Inorg. Chem.* **1990**, *38*, 97−200. (b) Kurtz, D. M., Jr. *Chem. Rev.* **1990**, *90*, 585−606.
(14) Rardin, R. L.; Tolman, W. B.; Lippard, S. J. *New J. Chem.* **1991**, *15*, 417−430.

0001-4842/96/0129-0190$12.00/0

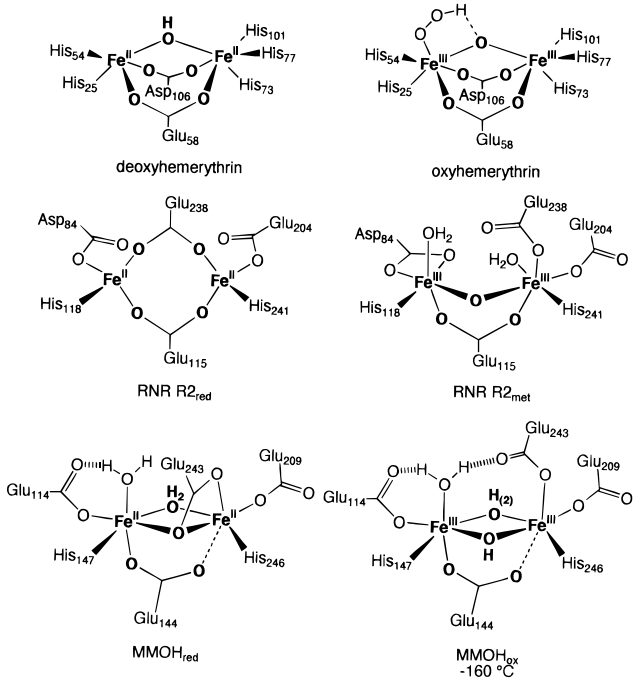

Figure 1. Diiron sites of hemerythrin (deoxyHr and oxyHr), ribonucleotide reductase (RNR $R2_{red}$ and RNR $R2_{met}$), and the hydroxylase component of methane monooxygenase ($MMOH_{red}$ and $MMOH_{ox}$).

reaction of O_2 with $MMOH_{red}$ first forms intermediate **P**, which then converts to intermediate **Q**. **Q** then reacts with methane to afford methanol and $MMOH_{ox}$, the diiron(III) form. On the basis of their spectroscopic properties, **P** and **Q** are proposed to be a (μ-peroxo)diiron(III) and a diiron(IV) species, respectively.[15,16] In corresponding studies with RNR R2, an intermediate **X** has been identified which is reduced to the diiron(III) state as it oxidizes Tyr122 to its radical form;[17] **X** thus contains one oxidizing equivalent above the diiron(III) oxidation state and is formally an $Fe^{III}Fe^{IV}$ species. Intermediate **X** presumably derives from the one-electron reduction of a diiron(III)−peroxide intermediate analogous to intermediate **P** in the MMOH cycle, but definitive evidence for such a species in the RNR R2 cycle is not yet available.

The accumulating evidence for intermediates in the oxygen activation chemistry of these non-heme diiron enzymes and the lack of structural information on these species have stimulated our efforts to provide synthetic inorganic precedents for these transient species in non-heme ligand environments. We have explored the reactions of diiron(II) complexes with O_2 or diiron(III) complexes with H_2O_2. To trap intermediates, we have used precursor complexes with vacant or labile sites to enhance formation of such species and low-temperature techniques to retard their decomposition and allow their characterization. This Account discusses two aspects of our work: (a) the design of a non-heme diiron−O_2 adduct and (b) the generation of high-valent bis(μ-oxo)diiron intermediates. These results have emboldened us to propose structures for the intermediates found in the MMOH and RNR R2 reaction cycles and formulate the working hypothesis shown in Figure 2 for a common oxygen activation mechanism for non-heme diiron enzymes.

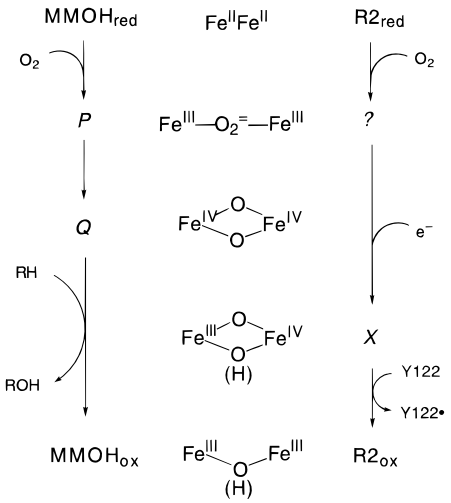

Figure 2. A common mechanistic framework for MMOH and RNR R2. The left and right columns are schemes summarizing results from single-turnover rapid kinetic studies of the reactions of O_2 with $MMOH_{red}$ (refs 15 and 16) and RNR $R2_{red}$ (ref 17), respectively. The middle column shows proposed structures for the observed intermediates based on a comparison of spectroscopic data on the enzyme intermediates and the transient species discussed in this Account.

Dioxygen Binding to a Diiron(II) Center

A number of bis(μ-carboxylato-*O,O′*)diiron(II) complexes have been structurally characterized and serve as models for the diiron(II) forms of the non-heme diiron enzymes including $[Fe_2(\mu\text{-OH})(OAc)_2(Me_3TACN)_2]X$ (modeling the deoxyHr core),[18,19] $[Fe_2(BIPhMe)_2(O_2CH)_4]$ (with a monodentate formate bridge, modeling the $MMOH_{red}$ core),[20] and $[Fe_2(TPA)_2(OAc)_2](BPh_4)_2$ (modeling the $R2_{red}$ core).[21] Exposure of these complexes to O_2 results in their oxidation, but no intermediate O_2 adduct has yet been detected in any of these cases. It is likely that the coordinative saturation of the Fe(II) ions in these complexes increases the barrier for the formation of the O_2 adduct relative to its decomposition by a subsequent reaction with another molecule of the precursor diiron(II) complex, thereby precluding the observation of an intermediate.

(15) (a) Lee, S.-K.; Nesheim, J. C.; Lipscomb, J. D. *J. Biol. Chem.* **1993**, *268*, 21569−21577. (b) Lee, S.-K.; Fox, B. G.; Froland, W. A.; Lipscomb, J. D.; Münck, E. *J. Am. Chem. Soc.* **1993**, *115*, 6450−6451.

(16) (a) Liu, K. E.; Wang, D.; Huynh, B. H.; Edmondson, D. E.; Salifoglou, A.; Lippard, S. J. *J. Am. Chem. Soc.* **1994**, *116*, 7465−7466. (b) Liu, K. E.; Valentine, A. M.; Qiu, D.; Edmondson, D. E.; Appelman, E. H.; Spiro, T. G.; Lippard, S. J. *J. Am. Chem. Soc.* **1995**, *117*, 4997−4998. (c) Liu, K. E.; Valentine, A. M.; Wang, D.; Huynh, B. H.; Edmondson, D. E.; Salifoglou, A.; Lippard, S. J. *J. Am. Chem. Soc.* **1995**, *117*, 10174−10185.

(17) (a) Bollinger, J. M., Jr.; Edmondson, D. E.; Huynh, B. H.; Filley, J.; Norton, J.; Stubbe, J. *Science* **1991**, *253*, 292−298. (b) Bollinger, J. M., Jr.; Tong, W. H.; Ravi, N.; Huynh, B. H.; Edmondson, D. E.; Stubbe, J. *J. Am. Chem. Soc.* **1994**, *116*, 8015−8023. (c) Bollinger, J. M., Jr.; Tong, W. H.; Ravi, N.; Huynh, B. H.; Edmondson, D. E.; Stubbe, J. *J. Am. Chem. Soc.* **1994**, *116*, 8024−8032. (d) Bollinger, J. M., Jr.; Stubbe, J.; Huynh, B. H.; Edmondson, D. E. *J. Am. Chem. Soc.* **1991**, *113*, 6289−6291. (e) Ravi, N.; Bollinger, J. M., Jr.; Huynh, B. H.; Edmondson, D. E.; Stubbe, J. *J. Am. Chem. Soc.* **1994**, *116*, 8007−8014. (f) Ravi, N.; Bominaar, E. L. *Inorg. Chem.* **1995**, *34*, 1040−1043.

(18) Chaudhuri, P.; Wieghardt, K. *Angew. Chem., Int. Ed. Engl.* **1985**, *24*, 778−779.

(19) Hartman, J. R.; Rardin, R. L.; Chaudhuri, P.; Pohl, K.; Wieghardt, K.; Nuber, B.; Weiss, J.; Papaefthymiou, G. C.; Frankel, R. B.; Lippard, S. J. *J. Am. Chem. Soc.* **1987**, *109*, 7387−7396.

(20) Tolman, W. B.; Liu, S.; Bentsen, J. G.; Lippard, S. J. *J. Am. Chem. Soc.* **1991**, *113*, 152−164.

(21) Ménage, S.; Zang, Y.; Hendrich, M. P.; Que, L., Jr. *J. Am. Chem. Soc.* **1992**, *114*, 7786−7792.

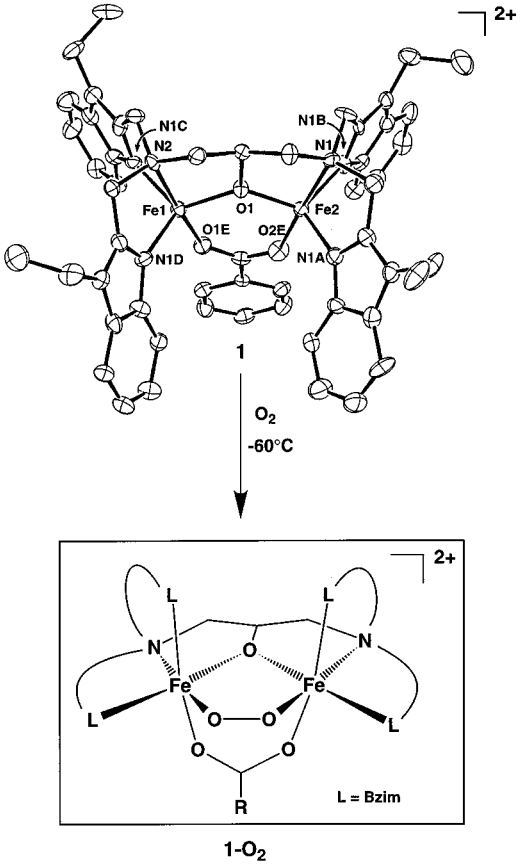

Figure 3. ORTEP plot for $[Fe_2(N\text{-Et-HPTB})(OBz)]^{2+}$ (**1**) and proposed structure for its dioxygen adduct (**1**$-O_2$). Adapted from ref 23.

We have used a dinucleating ligand with a 2-hydroxypropane backbone to afford diiron(II) complexes with available coordination sites. The crystal structure of $[Fe_2(N\text{-Et-HPTB})(OBz)](BF_4)_2$ (**1**) shows two Fe(II) centers with approximate trigonal bipyramidal geometry with amine nitrogens and carboxylate oxygens as axial ligands (Figure 3).[22,23] The corresponding complexes with pendant pyridine (**2**)[23] and 6-methylpyridine (**3**) ligands[24] have also been synthesized; these complexes constitute a family of coordinatively unsaturated diiron(II) complexes which readily form O_2 adducts.

Upon exposure to O_2 at -60 °C in CH_2Cl_2, the yellow solution of **1** turns a deep blue color (λ_{max} 588 nm, ϵ 1500 M^{-1} cm^{-1}).[22] The effect of O_2 is irreversible as no change is detected upon subsequent application of a vacuum. The blue complex is stable at -60 °C but decomposes readily to a diiron(III) species upon warming to ambient temperature. Manometric studies of O_2 uptake show that one O_2 molecule is taken up per mole of diiron(II) complex, indicating the formation of a 1:1 O_2 adduct. The related complex with pendant pyridines (**2**) also binds O_2 irreversibly,[23] but Suzuki et al. have found that the introduction of methyl groups at the 6-position of the pendant pyridines affords a complex (**3**) that reversibly binds O_2.[24] It appears likely that the 6-methyl groups introduce steric effects that shift the $Fe^{III/II}$ potentials more positive, thus achieving an equilibrium between the deoxy and oxy forms. Similar considerations apply to Kitajima's mononuclear $[Fe^{II}(Tp^{iPr2})(OBz)(CH_3CN)]$ complex, which forms a reversible 2:1 adduct with O_2.[25]

The resonance Raman spectrum of the blue **1**$-O_2$ adduct shows two resonance-enhanced vibrations at 476 and 900 cm^{-1}. These shift to 460 and 850 cm^{-1}, respectively, upon $^{18}O_2$ substitution[22,23] and are thus assigned to ν_{Fe-O} and ν_{O-O} modes. Similar results are obtained for the adducts of **2** and **3**. The ν_{O-O} values near 900 cm^{-1} appear typical of μ-1,2-peroxo complexes[26] including the O_2 adduct of $[Fe(Tp^{iPr2})(OBz)(CH_3CN)]$.[25]

The notion that dioxygen has been reduced to the peroxide oxidation level is confirmed by Mössbauer data on the **1**$-O_2$ adduct, which shows that the iron centers are oxidized to the high-spin iron(III) state (δ = 0.52 mm/s, ΔE_Q = 0.72 mm/s).[22] Furthermore, these iron(III) centers are in very similar, if not identical, environments and are antiferromagnetically coupled. The bridging carboxylate found in the precursor complex appears to remain bound in the O_2 adduct, as the λ_{max} for the adduct is sensitive to the nature of the bridging carboxylate. The use of propionate in place of benzoate results in a blue shift of the absorption maximum for the adduct to 570 nm,[22] consistent with the peroxo-to-iron(III) charge transfer nature of the transition. Taken together, the spectroscopic data implicate a (μ-alkoxo)(μ-1,2-peroxo)(μ-carboxylato)diiron(III) complex for the O_2 adduct (Figure 3), similar to that determined for $[Co_2(tpdb)(O_2)(CH_3COO)](PF_6)_2$.[27]

Some of the spectroscopic properties of **1**$-O_2$ are similar to those of MMOH peroxy intermediate **P**. For example, like **1**$-O_2$, **P** exhibits an absorption maximum near 600 nm (λ_{max} 625 nm, ϵ 1500 M^{-1} cm^{-1}) and a resonance-enhanced Raman vibration at 905 cm^{-1} that is sensitive to $^{18}O_2$ substitution.[16b,c] Furthermore, **P** has a diamagnetic ground state and shows only one Mössbauer doublet. These properties strongly suggest that **P** is a symmetric diiron(III)$-$peroxide complex. However, **P** has a significantly higher isomer shift (δ = 0.66 vs 0.52 mm/s), which is thus far reproduced only by (η^2-peroxo)iron(III) complexes such as $[Fe(OEP)O_2]^-$ [28] and the $[Fe^{III}(EDTA)]/H_2O_2$ adduct.[29] However, the ν_{O-O} values of these η^2-peroxo complexes are near 800 cm^{-1},[28,30] values significantly lower than that observed for **P**. Thus the precise dioxygen binding mode for **P** has not been established. Besides the μ-1,2-peroxo motif of **1**$-O_2$ (Figure 3), there are two other possible structures for a symmetric diiron-

(22) Ménage, S.; Brennan, B. A.; Juarez-Garcia, C.; Münck, E.; Que, L., Jr. *J. Am. Chem. Soc.* **1990**, *112*, 6423−6425.

(23) Dong, Y.; Ménage, S.; Brennan, B. A.; Elgren, T. E.; Jang, H. G.; Pearce, L. L.; Que, L., Jr. *J. Am. Chem. Soc.* **1993**, *115*, 1851−1859.

(24) (a) Hayashi, Y.; Suzuki, M.; Uehara, A.; Mizutani, Y.; Kitagawa, T. *Chem. Lett.* **1992**, 91−94. (b) Hayashi, Y.; Kayatani, T.; Sugimoto, H.; Suzuki, M.; Inomata, K.; Uehara, A.; Mizutani, Y.; Kitagawa, T.; Maeda, Y. *J. Am. Chem. Soc.* **1995**, *117*, 11220−11229.

(25) (a) Kitajima, N.; Fukui, H.; Moro-oka, Y.; Mizutani, Y.; Kitagawa, T. *J. Am. Chem. Soc.* **1990**, *112*, 6402−6403. (b) Kitajima, N.; Tamura, N.; Amagai, H.; Fukui, H.; Moro-oka, Y.; Mizutani, Y.; Kitagawa, T.; Mathur, R.; Heerwegh, K.; Reed, C. A.; Randall, C. R.; Que, L., Jr.; Tatsumi, K. *J. Am. Chem. Soc.* **1994**, *116*, 9071−9085.

(26) Brennan, B. A.; Chen, Q.; Juarez-Garcia, C.; True, A. E.; O'Connor, C. J.; Que, L., Jr. *Inorg. Chem.* **1991**, *30*, 1937−1943.

(27) Kayatani, T.; Hayashi, Y.; Suzuki, M.; Uehara, A. *Bull. Chem. Soc. Jpn.* **1994**, *67*, 2980−2989.

(28) (a) McCandlish, E.; Miksztal, A. R.; Nappa, M.; Sprenger, A. G.; Valentine, J. S.; Stong, J. D.; Spiro, T. G. *J. Am. Chem. Soc.* **1980**, *102*, 4268−4271. (b) Burstyn, J. N.; Roe, J. A.; Miksztal, A. R.; Shaevitz, B. A.; Lang, G.; Valentine, J. S. *J. Am. Chem. Soc.* **1988**, *110*, 1382−1388.

(29) Kauffmann, K.; Münck, E.; Dong, Y.; Que, L., Jr. Unpublished observations.

(30) Ahmad, S.; McCallum, J. D.; Shiemke, A. K.; Appelman, E. H.; Loehr, T. M.; Sanders-Loehr, J. *Inorg. Chem.* **1988**, *27*, 2230−2233.

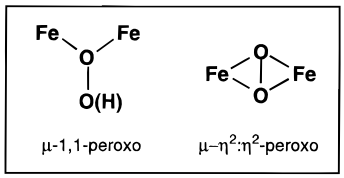

Figure 4. Alternative structures for a symmetric diiron(III)−peroxide intermediate.

(III)−peroxide complex (Figure 4),[16c,31] neither of which has yet been characterized in a diiron complex.

The O_2 adducts of **1** and **2** become unstable as the temperature is raised and are converted to diiron(III) complexes. The **1**$-O_2$ adduct decomposes in a first-order process, which is accelerated by the introduction of electron-donating substituents on the bridging benzoate.[32] It has been argued that these substituents increase the electron density at the metal centers, which would facilitate the cleavage of the O−O bond and stabilize higher oxidation states. When applied to protein active sites, this notion rationalizes why the carboxylate-rich diiron sites for MMOH and RNR R2 would promote dioxygen activation.

The symmetry of the adducts suggests that decomposition proceeds by homolysis of the O−O bond to afford highly reactive diiron(IV)−oxo species, although such an intermediate has not been observed. Perhaps the alkoxo bridge used in the design of the dinucleating ligand, while providing a framework to allow the formation and characterization of an O_2 adduct, is too rigid to allow the higher valent intermediate to be stabilized by an appropriate structural rearrangement. As will be seen in the next section, the use of the more flexible oxo bridge allows a higher valent species to be isolated.

High-Valent Non-Heme Iron Intermediates with $Fe_2(\mu\text{-}O)_2$ Cores

As discussed in the preceding section, the likelihood of observing an intermediate may be enhanced by using precursor complexes with vacant or labile sites. In model heme chemistry, the substitution of an axial halide with hydroxide facilitated the ligand exchange reaction with peracid and allowed the transient peroxide intermediate to be observed at low temperature.[33] We have thus synthesized the complexes $[Fe_2O(L)_2(OH)(H_2O)](ClO_4)_3$ (**4**) (L = TPA, 5-Me_3-TPA, or 5-Et_3-TPA).[34] The crystal structure of **4**(5-Et_3-TPA) shows one iron with a terminal hydroxide (r_{Fe2-O2} = 1.907 Å) and the other with an aqua ligand (r_{Fe1-O1} = 2.049 Å) with an O1−O2 separation of 2.464 Å (Figure 5). This distance suggests the presence of a hydrogen bond between the two oxygen atoms, which gives rise to an Fe−Fe separation of 3.346 Å and an Fe−O−Fe angle of 136.3.° Complex **4** can thus be considered a (μ-oxo)diiron complex with a novel supporting (H-O···H_2O)$^-$ bridge. Similar features are found in the structure of **4**(TPA).[35]

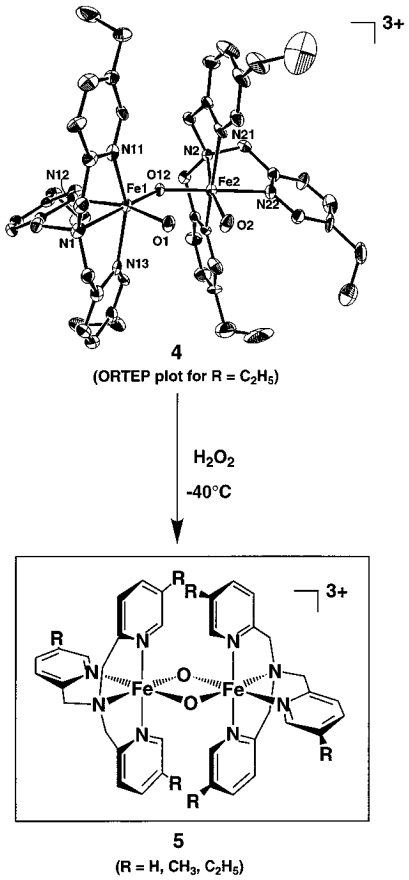

Figure 5. ORTEP plot for $[Fe_2O(5\text{-}Et_3\text{-}TPA)_2(OH)(H_2O)]^{3+}$, **4**(5-$Et_3$-TPA), and the proposed structure of the high-valent intermediate derived from the reaction of **4** with H_2O_2. Adapted from ref 34.

The reaction of **4** with H_2O_2 affords a high-valent intermediate in CH_3CN.[34,36] At room temperature, a flash of brilliant green color is observed upon mixing. When the reaction is carried out at −40 °C, this green intermediate (**5**) persists for 1−2 h in the case of L = TPA and longer for L = 5-Me_3-TPA, which allows the characterization of many of its unique spectroscopic properties. Intermediate **5** exhibits an intense visible absorption band with a maximum at 614−616 nm (Figure 6), a rhombic $S = {}^3/_2$ EPR spectrum with g = 4.45, 3.90, 2.01, and a Mössbauer doublet with δ = 0.14 mm/s, a value close to those found for Fe^{IV} complexes.[37] The TPA intermediate exhibits a resonance-enhanced (λ_{ex} 614 nm) Raman vibration at 666 cm^{-1}, while the corresponding 5-Me_3-TPA species shows a Fermi doublet at 656 and 676 cm^{-1} (Figure 6). These features shift to 638 (for L = TPA) and 634 (for L = 5-Me_3-TPA) cm^{-1} upon the addition of $H_2{}^{18}O$ but are insensitive to D_2O. Two arguments exclude the possibility that the chromophore arises from a peroxide adduct, as may be initially suspected: (a) the

(31) Ling, J.; Sahlin, M.; Sjöberg, B.-M.; Loehr, T. M.; Sanders-Loehr, J. *J. Biol. Chem.* **1994**, *269*, 5595−5601.
(32) Dong, Y.; Yan, S.; Young, V. G., Jr.; Que, L., Jr. *Angew. Chem., Int. Ed. Engl.*, in press.
(33) Groves, J. T.; Watanabe, Y. *J. Am. Chem. Soc.* **1988**, *110*, 8443.
(34) Dong, Y.; Fujii, H.; Hendrich, M. P.; Leising, R. A.; Pan, G.; Randall, C. R.; Wilkinson, E. C.; Zang, Y.; Que, L., Jr.; Fox, B. G.; Kauffmann, K.; Münck, E. *J. Am. Chem. Soc.* **1995**, *117*, 2778−2792.
(35) Hazell, A.; Jensen, K. B.; McKenzie, C. J.; Toflund, H. *Inorg. Chem.* **1994**, *33*, 3127−3134.
(36) Leising, R. A.; Brennan, B. A.; Que, L., Jr.; Fox, B. G.; Münck, E. *J. Am. Chem. Soc.* **1991**, *113*, 3988−3990.
(37) (a) Mandon, D.; Weiss, R.; Jayaraj, K.; Gold, A.; Terner, J.; Bill, E.; Trautwein, A. X. *Inorg. Chem.* **1992**, *31*, 4404−4409. (b) Vogel, E.; Will, S.; Tilling, A. S.; Neumann, L.; Lex, J.; Bill, E.; Trautwein, A. X.; Wieghardt, K. *Angew. Chem., Int. Ed. Engl.* **1994**, *33*, 731−735. (c) Jüstel, T.; Weyhermüller, T.; Wieghardt, K.; Bill, E.; Lengen, M.; Trautwein, A. X.; Hildebrandt, P. *Angew. Chem., Int. Ed. Engl.* **1995**, *34*, 669−672. (d) Summerville, D. A.; Cohen, I. A. *J. Am. Chem. Soc.* **1976**, *98*, 1747−1752. (e) Collins, T. J.; Fox, B. G.; Hu, Z. G.; Kostka, K. L.; Münck, E.; Rickard, C. E. F.; Wright, L. J. *J. Am. Chem. Soc.* **1992**, *114*, 8724−8725. (f) Schulz, C. E.; Rutter, R.; Sage, J. T.; Debrunner, P. G.; Hager, L. P. *Biochemistry* **1984**, *23*, 4743−4754.

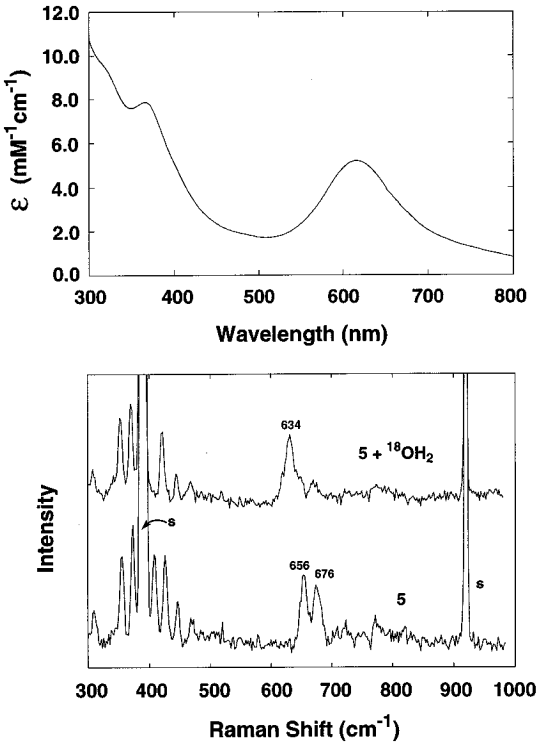

Figure 6. Upper panel: electronic spectrum of **5**(5-Me_3-TPA) in CH_3CN at −40 °C. Lower panel: resonance Raman spectra of **5**(5-Me_3-TPA) in CH_3CN at ∼80 K with laser excitation at 614 nm. Raman vibrations found in the 320−500 cm^{-1} region are associated with other metal−ligand vibrations. Adapted from ref 34.

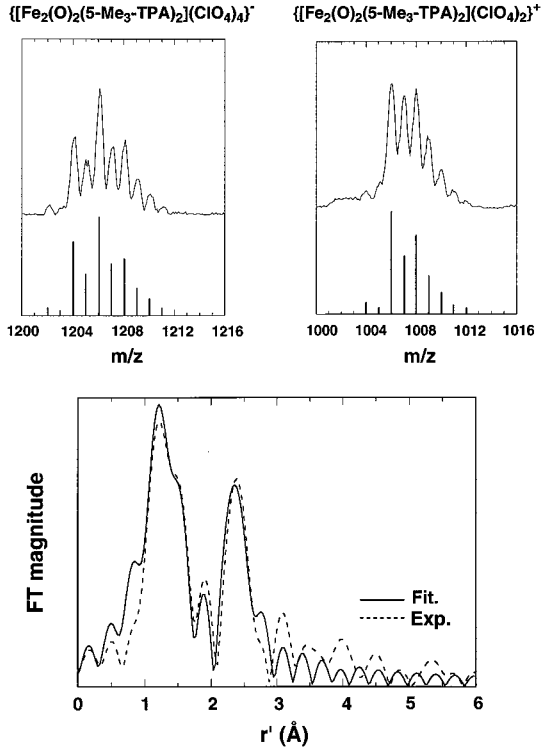

Figure 7. Upper panel: electrospray ionization mass spectra of **5**(5-Me_3-TPA) in cold CH_3CN (dry ice on the syringe). Lower panel: Fourier transformed EXAFS data ($k = 2-13$ $Å^{-1}$) of **5**(5-Me_3-TPA). Adapted from ref 34.

frequency of this vibration being significantly lower than that normally observed for the ν_{O-O} of peroxides (750−900 cm^{-1}),[22-26] and (b) the sensitivity of the vibration to $H_2{}^{18}O$ exchange. The ∼30 cm^{-1} shift observed in $H_2{}^{18}O$ is nearly identical to the calculated isotope shift of 29 cm^{-1} for a diatomic Fe−O unit, strongly suggesting its assignment to ν_{Fe-O}. This 666 cm^{-1} value, however, is intermediate between those observed for Fe−O single bonds (400−500 cm^{-1})[38] and those found for Fe−O double bonds (800−850 cm^{-1}).[39]

The elucidation of the nature of **5** has been greatly facilitated by the isolation of a solid at low temperatures.[34] Though **5** was initially proposed to be a mononuclear species,[40] subsequent studies on solid **5**(5-Me_3-TPA) demonstrated it to have the formula $[Fe_2O_2(5\text{-}Me_3\text{-}TPA)_2](ClO_4)_3$. Its elemental analysis shows a 1:1:1.5 ratio of Fe:5-Me_3-TPA:ClO_4, and its electrospray ionization mass spectra exhibit prominent peaks with masses and isotope distribution patterns consistent with the presence of the ions $\{[Fe_2O_2(5\text{-}Me_3\text{-}TPA)_2](ClO_4)_2\}^+$ and $\{[Fe_2O_2(5\text{-}Me_3\text{-}TPA)_2](ClO_4)_4\}^-$ (Figure 7). The EXAFS spectrum of **5**(5-Me_3-TPA) reveals how the Fe_2O_2 unit is arranged. There is a prominent feature at $r' = 2.5$ Å that can only be fitted with an Fe scatterer at 2.89 Å (Figure 7), a distance consistent with the presence of an $Fe_2(\mu\text{-}O)_2$ core. Similar metal−metal distances have been found in $[Fe^{III}_2(\mu\text{-}O)_2(6\text{-}Me_3\text{-}TPA)_2](ClO_4)_2$ (2.72 Å), the only structurally characterized complex with an $Fe_2(\mu\text{-}O)_2$ core,[41] as well as in the more common bis(μ-oxo)dimanganese complexes.[42] These $Mn_2O_2{}^{3+}$ complexes exhibit a ca. 700 cm^{-1} Raman feature that is associated with a breathing mode of the $Mn_2(\mu\text{-}O)_2$ core.[43] Viewed in this light, the 666 cm^{-1} Raman vibration observed for **5** can now be assigned to a vibration of the $Fe_2(\mu\text{-}O)_2$ core.

The +3 charge on the Fe_2O_2 core implies a formal $Fe^{III}Fe^{IV}$ oxidation state, and the complex thus contains one oxidizing equivalent above the diiron(III) state. In agreement with this notion, 1 equiv of ferrocene reduces **5**(5-Me_3-TPA) to the diiron(III) state, while cyclic voltammetry of **5**(5-Me_3-TPA) in CH_3CN at −40 °C shows a quasi-reversible one-electron wave at +960 mV vs NHE for the $[Fe^{III}Fe^{IV}/Fe^{III}Fe^{III}]$ couple. Furthermore, the K-edge energy of **5**(5-Me_3-TPA) is 3 eV higher than that of the precursor diiron(III) complex **4**(5-Me_3-TPA). Since **5** shows only one sharp quadrupole doublet in its Mössbauer spectrum, the two iron sites must be equivalent, so a localized Fe^{III}-Fe^{IV} description can be ruled out. In order to account for the structural and electronic equivalence of the two sites as well as the $S = {}^3/_2$ ground state, we presently favor a valence-delocalized model derived from the double exchange coupling of a low-spin ($S_1 = {}^1/_2$) Fe(III) and a low-spin ($S_2 = 1$) Fe(IV) center.[34]

(38) (a) Sanders-Loehr, J.; Wheeler, W. D.; Shiemke, A. K.; Averill, B. A.; Loehr, T. M. *J. Am. Chem. Soc.* **1989**, *111*, 8084−8093. (b) Reed, R. A.; Rodgers, K. R.; Kushmeider, K.; Spiro, T. G.; Su, Y. O. *Inorg. Chem.* **1990**, *29*, 2881−2883.

(39) (a) Proniewicz, L. M.; Bajdor, K.; Nakamoto, K. *J. Phys. Chem.* **1986**, *90*, 1760−1766. (b) Paeng, K.; Kincaid, J. R. *J. Am. Chem. Soc.* **1988**, *110*, 7913−7915. (c) Kincaid, J. R.; Schneider, A. J.; Paeng, K. *J. Am. Chem. Soc.* **1989**, *111*, 735−737.

(40) Problems with the quantitative corrrelation of the $S = {}^3/_2$ EPR signal of **5**(TPA) with the Mössbauer component corresponding to **5**(TPA) led to the incorrect interpretation.[34,36]

(41) (a) Zang, Y.; Dong, Y.; Que, L., Jr.; Kauffmann, K.; Münck, E. *J. Am. Chem. Soc.* **1995**, *117*, 1169−1170. (b) Zang, Y.; Pan, G.; L. Que, J.; Fox, B.; Münck, E. *J. Am. Chem. Soc.* **1994**, *116*, 3653−3654.

(42) Wieghardt, K. *Angew. Chem., Int. Ed. Engl.* **1989**, *28*, 1153−1172.

(43) (a) Czernuszewicz, R. S.; Dave, B.; Rankin, J. G. In *Spectroscopy of Biological Molecules*; Hester, R. E., Girling, R. B., Eds.; Royal Society of Chemistry: Cambridge, 1991; pp 285−288. (b) Dave, B. C.; Czernuszewicz, R. S. *Inorg. Chim. Acta* **1994**, *227*, 33−41. (c) Gamelin, D. R.; Kirk, M. L.; Stemmler, T. L.; Pal, S.; Armstrong, W. H.; Penner-Hahn, J. E.; Solomon, E. I. *J. Am. Chem. Soc.* **1994**, *116*, 2392−2399.

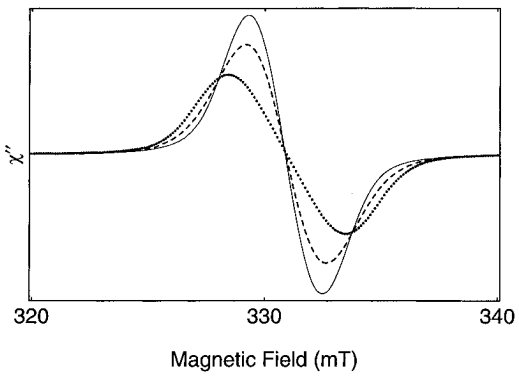

Figure 8. EPR spectra of **6**(6-Me-TPA) in CH_3CN (—, ^{56}Fe, ^{16}O; – – –, ^{56}Fe, ^{17}O; ···, ^{57}Fe, ^{16}O). Reprinted with permission from ref 44. Copyright 1995 American Chemical Society.

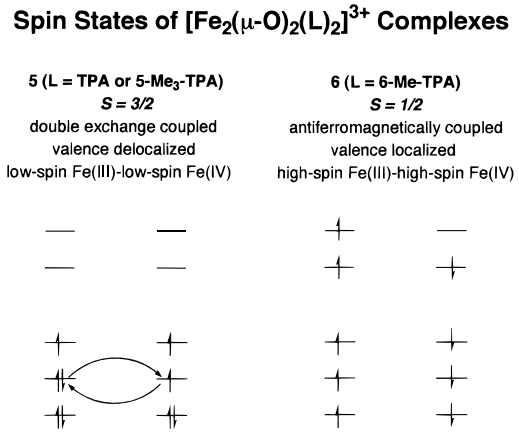

Figure 9. Scheme illustrating spin coupling interactions in **5** and **6**.

Additional support for this electronic description of **5** has been obtained from the synthesis of $[Fe_2(O)_2(6\text{-Me-TPA})_2]^{3+}$ (**6**), a new member of the $[Fe_2(O)_2L_2]^{3+}$ series.[44] Complex **6** differs from **5** in electronic structure. It has an $S = {}^1/_2$ ground state which gives rise to an isotropic EPR signal at $g = 2.0$. This EPR signal is broadened by the introduction of ^{57}Fe and ^{17}O (from $H_2{}^{17}O$), showing that the unpaired spin is associated with the Fe_2O_2 core (Figure 8). The Mössbauer spectrum of **6** shows two quadrupole doublets with $\delta = 0.48$ and 0.08 mm/s corresponding to the high-spin Fe^{III} and Fe^{IV} sites, respectively, that couple antiferromagnetically to the $S = {}^1/_2$ ground state. Intermediate **6** differs in structure from **5**(TPA) in having a 6-methyl group on one pyridine of each TPA ligand. The presence of the 6-methyl substituent prevents formation of the shorter $Fe-N_{pyridine}$ bond required by a low-spin iron center, which typically has an ionic radius about 0.2 Å smaller than the corresponding high-spin center. For example, $[Fe^{III}(TPA)acac]^{2+}$ is low spin, while $[Fe^{III}(6\text{-Me-TPA})acac]^{2+}$ is high spin.[44,45] The different spin coupling schemes ascribed to **5** and **6** are illustrated in Figure 9.

We have thus characterized two types of $[Fe_2(O)_2]^{3+}$ complexes, and their properties have some resemblance to MMOH intermediate **Q** and RNR R2 intermediate **X**. Intermediate **Q** exhibits a Mössbauer doublet ($\delta \sim 0.17$ mm/s; $\Delta E_Q \sim 0.57$ mm/s) whose behavior in high applied field indicates that it has a diamagnetic ground state;[15b,16a,c] on the basis of these properties, **Q** has been proposed to be an antiferromagnetically coupled diiron(IV) species.[15b] Its rather unique Mössbauer parameters are surprisingly quite similar to those of **5**, despite the fact that **5** contains one more reducing equivalent. Whether this similarity is a mere coincidence or has some further chemical significance remains to be established.

Intermediate **X**, like **6**, also exhibits an isotropic $S = {}^1/_2$ EPR signal which is broadened by the introduction of ^{57}Fe and ^{17}O (from $^{17}O_2$ and $H_2{}^{17}O$).[17] Its Mössbauer spectrum consists of two components; one site ($\delta = 0.55$ mm/s) clearly possesses high-spin iron(III) character, and the other has a lower isomer shift indicative of an oxidation state intermediate between high-spin Fe^{III} and Fe^{IV}. Originally these properties were interpreted to indicate the presence of a diiron(III) unit coupled to a ligand radical.[17] However, the similarity in the EPR properties of **X** and **6** has led us to propose that an $Fe^{III}Fe^{IV}$ formulation be considered to describe **X**.[44] Indeed recent ENDOR results on **X** indicate that one of the iron sites in **X** has Fe^{IV} character.[46]

A Common Oxygen Activation Mechanism for Non-Heme Diiron Enzymes

The intermediates we have described in this Account provide the basis for proposing a common mechanistic framework (Figure 2) for activating dioxygen at the non-heme diiron centers of MMOH and RNR R2. While this mechanism incorporates features that others have proposed in earlier papers,[3,5,47] our biomimetic studies have provided many of the synthetic precedents for the structures postulated in the scheme. This mechanism consists of (a) the initial interaction of O_2 with the diiron(II) center forming a symmetric diiron(III) peroxide adduct (see Figures 3 and 4 for possible structures); (b) the homolysis of the peroxide O−O bond to form a bis(μ-oxo)diiron(IV) species; and (c) the reduction of this high-valent species to the diiron(III) state in two one-electron steps via an Fe^{III}-Fe^{IV} species.

The bis(μ-oxo)diiron core plays a key role in our proposed mechanism. In heme enzymes, the key oxidant is an oxoiron(IV) porphyrin radical intermediate, the two oxidizing equivalents being stored in the Fe^{IV} center and in the porphyrin ligand. For non-heme diiron enzymes, the two oxidizing equivalents are proposed to be stored in the diiron(IV) center, the second iron replacing the porphyrin as the second storage site, with the oxo bridges contributing to the stabilization of the diiron(IV) oxidation state.

The involvement of the two metal centers in dioxygen binding and activation has significant mechanistic implications. The monometallic nature of the heme active site requires the heterolytic cleavage of the O−O bond to avoid formation of the hyper-reactive hydroxyl radical. Consequently Nature has evolved an elaborate push-pull apparatus to promote O−O bond heterolysis.[48] Such an apparatus would not necessarily be required for a diiron active site, particularly with a symmetric diiron(III)−peroxo species

(44) Dong, Y.; Que, L., Jr.; Kauffmann, K.; Münck, E. *J. Am. Chem. Soc.* **1995**, *117*, 11377−11378.
(45) Zang, Y.; Dong, Y.; Kim, J.; Que, L., Jr. Results to be published.
(46) Burdi, D.; Sturgeon, B. E.; Tong, W. H.; Stubbe, J.; Hoffman, B. M. *J. Am. Chem. Soc.* **1996**, *118*, 281−282.
(47) (a) Shteinman, A. A. *FEBS Lett.* **1995**, *362*, 5−9. (b) Que, L., Jr. *Science* **1991**, *253*, 273−274.
(48) Dawson, J. H. *Science* **1988**, *240*, 433−439.

as appears to be the case for MMOH,[16b,c] because the diiron(IV) state can be readily attained by homolysis of the O−O bond. Precedent for such an O−O homolysis has recently been demonstrated by Tolman et al. for a (μ-η^2:η^2-peroxo)dicopper species converting to a bis(μ-oxo)dicopper species.[49]

The intermediates described in this Account provide strong support for the proposed mechanistic framework in Figure 2. In particular, the $[Fe_2(O)_2L_2]^{3+}$ species are to date the only characterized synthetic examples of high-valent bis(μ-oxo)diiron species.[50] Complexes **5** and **6** are formally in the $Fe^{III}Fe^{IV}$ oxidation state and thus correspond to enzyme intermediates such as RNR R2 intermediate **X**. Indeed **6** approximates the spectroscopic properties of **X**,[44] and **5** has been demonstrated to oxidize phenol to its radical form.[52] Though it contains one less oxidizing equivalent than MMOH intermediate **Q**, **5** can hydroxylate an aliphatic C−H bond as well, in this case, the oxidation of cumene to cumyl alcohol.[52] While the C−H bond of cumene is substantially weaker than that of methane, the oxidation is an analogous reaction. Presumably the corresponding $Fe^{IV}Fe^{IV}$ derivative of **5** should have a higher potential and thus the greater oxidizing power to react with substrates having stronger C−H bonds.

The presence of a bis(μ-oxo)diiron core has yet to be demonstrated for any of the enzyme intermediates thus far characterized. However, the synthetic precedents we have described in this Account make this mechanistic scheme quite plausible. The very existence of these bis(μ-oxo)diiron complexes and the similarity of their spectroscopic and reactivity properties to those of the enzyme intermediates provide strong support that related species are very likely to participate in the oxygen activation mechanisms of MMOH and RNR R2 as well as those of newer members of this class[53] such as stearoyl ACP Δ^9-desaturase, toluene 4-monooxygenase, and phenol hydroxylase.

Note Added in Proof: After this paper was accepted, Ookubo et al. reported the crystal structure of a reversible diiron−O_2 adduct with a structure similar to that of **1**−O_2 proposed in Figure 3 (Ookubo, T.; Sugimoto, H.; Nagayama, T.; Masuda, H.; Sato, T.; Tanaka, K.; Maeda, Y.; Okawa, H.; Hayashi, Y.; Uehara, A.; Suzuki, M. *J. Am. Chem. Soc.* **1996**, *118*, 701−702). The structures of two other adducts have also been solved: $[Fe_2(N\text{-}Et\text{-}HPTB(O_2)(OPPh_3)_2]^{3+}$ (ref 32) and $[Fe_2(Tp^{iPr2})_2(O_2CCH_2Ph)_2(O_2)]$ (Kim, K.; Lippard, S. J. Submitted for publication).

The modeling studies related in this Account were supported by the National Institutes of Health (GM-38767).

AR950146G

(49) (a) Mahapatra, S.; Halfen, J. A.; Wilkinson, E. C.; Pan, G.; Cramer, C. J.; Que, L., Jr.; Tolman, W. B. *J. Am. Chem. Soc.* **1995**, *117*, 8865−8866. (b) Mahapatra, S.; Halfen, J. A.; Wilkinson, E. C.; Que, L., Jr.; Tolman, W. B. *J. Am. Chem. Soc.* **1994**, *116*, 9785−9786. (c) Halfen, J. A.; Mahapatra, S.; Wilkinson, E. C.; Kaderli, S.; Young, V. G., Jr.; Que, L., Jr.; Zuberbühler, A. D.; Tolman, W. B. *Science*, in press.

(50) Two other formally $Fe^{III}Fe^{IV}$ complexes are known, $[Fe(TPP)]_2N$[51] and $[Fe(Cl_4Cat)(Me_3TACN)]_2N$.[37c] Both are crystallographically characterized and have μ-nitrido bridges

(51) Scheidt, W. R.; Summerville, D. A.; Cohen, I. A. *J. Am. Chem. Soc.* **1976**, *98*, 6623−6628.

(52) Kim, C.; Dong, Y.; Que, L., Jr. Results to be published.

(53) (a) Fox, B. G.; Shanklin, J.; Somerville, C.; Münck, E. *Proc. Natl. Acad. Sci. U.S.A.* **1993**, *90*, 2486−2490. (b) Fox, B. G.; Shanklin, J.; Ai, J.; Loehr, T. M.; Sanders-Loehr, J. *Biochemistry* **1994**, *33*, 12776−12786.